NGU REPORT 2022.013

Helicopter-borne magnetic, electro-magnetic and radiometric geophysical survey in Øksfjord peninsula, Troms and Finnmark Counties

GEOLOGY FOR SOCIETY

SINCE 1858

GEOLOGICAL SURVEY OF NORWAY

- NGU -

NGU REPORT
2022.013

Helicopter-borne magnetic, electro-magnetic and radiometric geophysical survey in Øksfjord peninsula, Troms and Finnmark Counties

NORGES GEOLOGISKE UNDERSØKELSE
- NGU -

REPORT

Geological Survey of Norway
P.O.Box 6315 TORGARDEN
NO-7491 TRONDHEIM
Tel.: 47 73 90 40 00

Report no.: 2022.013

ISSN: 0800-3416 (print)
ISSN: 2387-3515 (online)

Grading: Open

Title: Helicopter-borne magnetic, electro-magnetic and radiometric geophysical survey in Øksfjord area, Troms and Finnmark counties.

Authors:
Frode Ofstad and Alexandros Stampolidis

Client:
NGU

County:
Troms and Finnmark

Municipality:
Kvænangen, Loppa, Alta, Troms og Finnmark

Map-sheet name (M=1:250.000)
Troms, Finnmark

Map-sheet no. and -name (M=1:50.000)
1735-1/2/3/4

Deposit name and grid-reference:
WGS84 UTM34N 530000E, 7780000N

Number of pages: 32 **Price (NOK):** 120
Map enclosures:

Fieldwork carried out:	**Date of report:**	**Project no.:**	**Person responsible:**
Sept 2014 and Aug 2019	**March 2022**	388900	Marco Brönner

Summary:

NGU conducted an airborne geophysical survey in Øksfjord area, in Kvænangen, Loppa og Alta municipalities in Troms and Finnmark, as part of NGU's general airborne mapping program. The data acquisition in the Øksfjord area was carried out from 20th to 31st of August 2019. Two flights from the same area, flown September 1st, 2014, were also included in the data set for processing and presentation.

This report describes and documents the acquisition, processing and visualization of the acquired datasets and presents them in maps. The geophysical surveys consist of 2155 line-km data, covering an area of 813 km^2, with 245 km (49km^2) flown in 2014 from Ystneset, near Øksfjord community center, and 1910 km (764 km^2) flown in 2019 from Alteidet.

NGU's modified Geotech Ltd. Hummingbird frequency domain EM system supplemented by an optically pumped Cesium magnetometer and the Radiation Solutions 1024 channels RSX-5 spectrometer mounted on a AS350-B3 helicopter were used for data acquisition.

Collected data were processed at NGU using Geosoft Oasis Montaj software. Raw total magnetic field data were corrected for diurnal variation and leveled using a micro-levelling algorithm. Radiometric data were processed using standard procedures as recommended by International Atomic Energy Association (IAEA).

EM data were filtered and leveled using both automated and manual levelling procedures. Apparent resistivity was calculated from in-phase and quadrature data for three coplanar frequencies (880Hz, 6.6kHz and 34kHz), and for two coaxial frequencies (980Hz and 7kHz) separately using a homogeneous half space model.

All data were gridded using cell size of 100x100 meters and presented as 40% transparent grids with shaded relief on top of topographic maps.

Keywords:	**Airborne**	**Geophysics**
Magnetic	**Gamma-ray spectrometry**	**Radiometric**
Electromagnetic	**Technical report**	

CONTENTS

FIGURES

TABLES

INTRODUCTION

In 2019 NGU received government funds to acquire airborne geophysical data from northern Norway. The helicopter survey presented in this report covers most of the western part of Øksfjord peninsula, and contain data measured by NGU in 2014 and 2019. The processed data amounts to 2155 line-km, or 813 km^2, with the area measured in 2014 shown inside the orange lines, and data from 2019 inside red lines, in Figure 1.

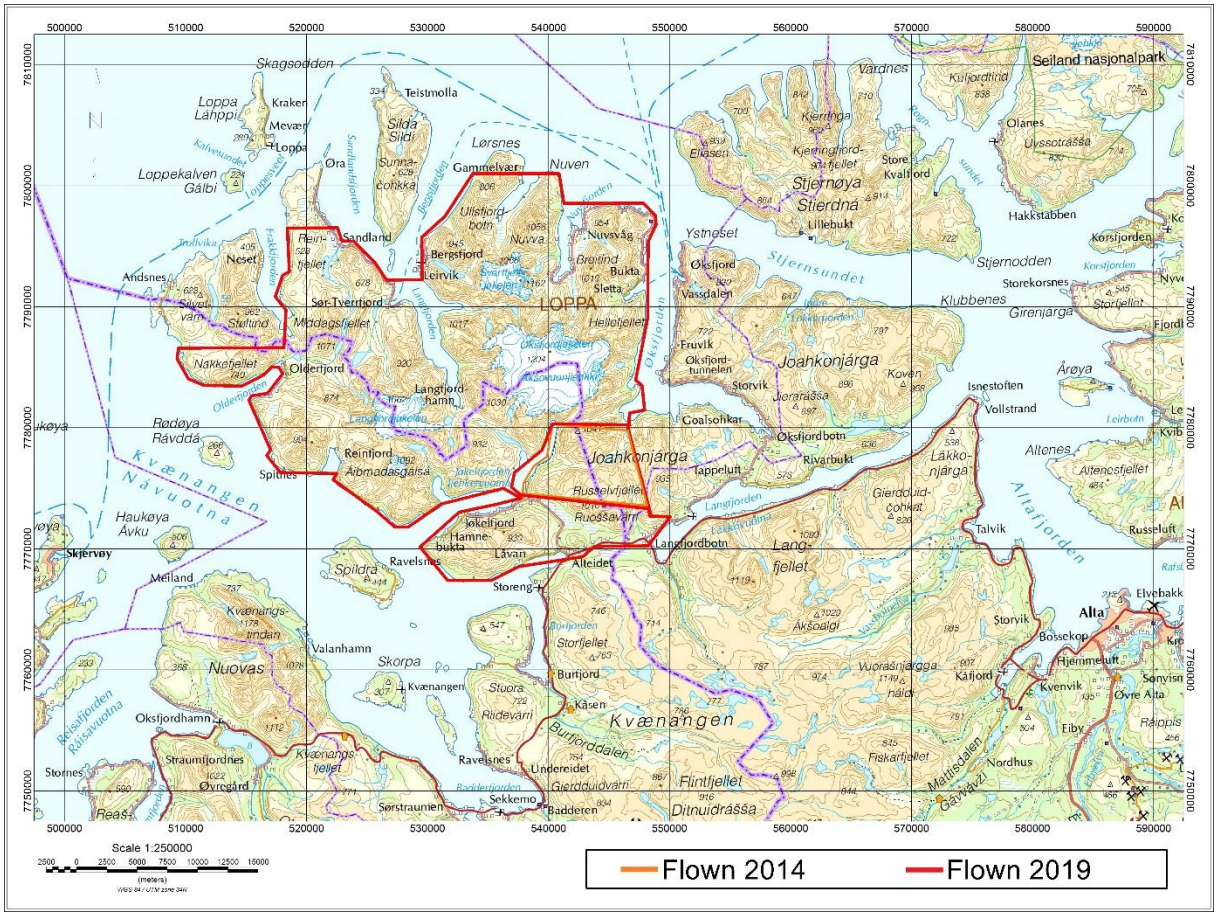

Figure 1: Helicopter survey area in Øksfjord peninsula.

Table 1. Flight specifications

Survey name	Surveyed lines (km)	Surveyed area (Km^2)	Line direction	Line Separation	Average speed (km/h)
Øksfjord 2019	1910	764	90	400	74
Øksfjord 2014	245	49	96	200	50
Total Area	2155	813			70

The east part of Øksfjord peninsula was mapped by NGU in 2013, and the surrounding ocean area was surveyed with fixed-wing aircraft during the TROFI survey in 2014.

The objective of the airborne geophysical survey was to obtain a dense high-resolution magnetic, electromagnetic, and radiometric data set over the survey area. This data is required for the enhancement of a general understanding of the regional geology of the area, with adjoining areas covered by airborne surveys from earlier years.

In this regard, the new data can be used to map contacts and structural features within the survey area. It also improves defining the potential of known zones of mineralization, their geological settings, and identifying new areas of interest, as the dataset fills a gap in the high-resolution geophysical surveys of the region.

The survey incorporated the use of a Hummingbird™ 5-frequency electromagnetic (EM) system supplemented by a high-sensitivity cesium magnetometer, gamma-ray spectrometer, and a helicopter mounted radar altimeter. A GPS navigation computer system with flight path indicators ensured accurate positioning of the geophysical data with respect to the World Geodetic System 1984 geodetic datum (WGS-84).

1. SURVEY SPECIFICATIONS

1.1 Airborne survey parameters

NGU used a modified Hummingbird™ EM and magnetic helicopter survey system designed to obtain low level, slow speed, detailed airborne EM, and magnetic data (Geotech 1997). The system was supplemented by a Radiation Solutions RSX-5, 1024 channel gamma-ray spectrometer, installed under the main body of the helicopter, used to map ground concentrations of U, Th and K, and radiation Total Counts.

Two flights were flown September 1st, 2014, from Ystneset, near Øksfjord community center. The survey was later completed from August 21st to 31st 2019 from the base in Alteidet. A Eurocopter AS350-B3 (LN-OGL) from helicopter company HeliScan AS was used during the survey. The 2019 survey lines were spaced 400 meters apart, with lines oriented at 90° in UTM zone 34. The 2014 survey lines were spaced 200 meters apart, with lines oriented at 90° in UTM zone 35, or 96° in UTM 34. The magnetic and electromagnetic sensors are housed in a single 7 meters long bird, towed 30 meters below the helicopter, flown at an average of 83 meters above the topographic surface.

Rugged terrain and abrupt changes in topography affected the aircraft pilot's ability to 'drape' the terrain, meaning the average instrumental height was sometimes higher than the standard survey instrumental height, which is defined as 30 meters plus a height of obstacles (trees, power lines etc.) for EM and magnetic sensors.

The ground speed of the aircraft varied from 20 to 130 km/h depending on topography, wind direction and its magnitude. On average the ground speed during measurements is calculated to 70 km/h. Magnetic data were recorded at 0.2 second intervals resulting in approximately 4 meters average point spacing.

EM data were recorded at 0.1 second intervals resulting in data with a sample increment of 2 meters along the ground in average. Spectrometry data were recorded every 1 second giving a point spacing of approximately 20 meters. The above parameters allow sufficient detail recognition in the data to detect subtle anomalies that may represent mineralization and/or rocks of different lithological and petrophysical composition.

A base magnetometer to monitor diurnal variations in the magnetic field was located at the base at Alteidet in 2019, and at the base near Ystneset in 2014. The GEM GSM-19 base magnetometer data were recorded once every 3 seconds. The CPU clock of the base magnetometer and the helicopter magnetometer were both synchronized to UTC (Universal Time Coordinates) through the built-in GPS receiver to allow correction of diurnals.

Navigation system uses GPS/GLONASS satellite tracking systems to provide real-time WGS-84 coordinate locations for every second. The accuracy achieved with no differential corrections is reported to be ± 5 meters in the horizontal directions. The GPS receiver antenna was mounted internally inside the canopy of the helicopter.

For quality control, the electromagnetic, magnetic, and radiometric, altitude and navigation data were monitored on four separate windows in the operator's display during flight, while they were recorded in three data ASCII streams to the PC hard disk drive. Spectrometry data were also recorded on an internal hard drive of the spectrometer. The data files were transferred to the field workstation via USB flash drive. The raw data files were backed up onto USB flash drive in the field.

1.2 Airborne survey instrumentation

Instrument specifications are given in Table 2. Frequencies and coil configurations for the Hummingbird EM system are given in Table 3.

Table 2. Instrument Specifications

Instrument	Producer/Model	Accuracy / Sensitivity	Sampling frequency / interval
Magnetometer	Scintrex Cs-2	<2.5nT throughout range / 0.0006nT √Hz rms	5 Hz
Base magnetometer	GEM GSM-19	0.1 nT	3 s
Electromagnetic	Geotech Hummingbird	1 – 2 ppm	10 Hz
Gamma spectrometer	Radiation Solutions RSX-5	1024 channels, 16 liters down, 4 liters up	1 Hz
Radar altimeter	Bendix/King KRA 10A	± 5 ft 40 – 100 feet ± 5 % 100 – 500 feet ± 7 % 500 – 2500 feet	1 Hz
Pressure/temperature	Honeywell PPT	± 0.03 % FS	1 Hz
Navigation	Topcon GPS-receiver	± 5 meters	1 Hz
Acquisition system	NGU custom software		

Figure 2: HeliScan helicopter and Hummingbird system on the ground in Ystneset, Øksfjord

Table 3. Hummingbird EM system, frequency, and coil configurations

Coils	Frequency	Orientation	Separation
A	7700 Hz	Coaxial	6.30 m
B	6600 Hz	Coplanar	6.30 m
C	980 Hz	Coaxial	6.025 m
D	880 Hz	Coplanar	6.025 m
E	34133 Hz	Coplanar	4.90 m

1.3 Airborne Survey Logistics Summary

A summary of the survey specifications is shown in Table 4.

Table 4. Survey specifications summary

Parameter	Specifications
Traverse (survey) line spacing	200 meters
Traverse line direction	E-W (90º)
Nominal aircraft ground speed	20 - 130 km/h
Average aircraft ground speed	70 km/h
Average sensor terrain clearance Mag	83 meters
Average sensor terrain clearance Rad	113 meters
Sampling rates:	
Magnetometer	0.2 seconds
Electromagnetic system	0.1 seconds
Spectrometer, GPS, altimeter	1.0 second
Base Magnetometer	3.0 seconds

2. DATA PROCESSING AND PRESENTATION

Data acquisition was done by Alexandros Stampolidis in 2014 and Frode Ofstad in 2019. The magnetic, spectrometry and all resistivity data were processed by Frode Ofstad at NGU. The ASCII data files were loaded into three separate Oasis Montaj databases. The datasets were processed consequently according to processing flow charts shown in Appendix A1, A2 and A3.

2.1 Total Field Magnetic Data

At the first stage the raw magnetic data were visually inspected, and spikes were removed manually. Non-linear filter was also applied to airborne raw data to eliminate short-period spikes. Typically, several corrections must be applied to magnetic data before gridding - heading correction, lag correction and diurnal correction.

Diurnal corrections

The temporal fluctuations in the magnetic field of the earth affect the total magnetic field readings recorded during the airborne survey. This is commonly referred to as the magnetic diurnal variation. These fluctuations can be effectively removed from the airborne magnetic dataset by using a stationary reference magnetometer that records the magnetic field of the earth simultaneously with the airborne sensor at given short time interval.

Diurnal variation data were inspected for spikes, and spikes were removed manually if necessary. Magnetic diurnals that were recorded on the base station magnetometer were within the standard NGU specifications during the entire survey (Rønning 2013).

Diurnal variations were measured with GEM GSM-19 magnetometer. The base station computer clock was continuously synchronized with GPS clock. The recorded data are merged with the airborne data and the diurnal correction is applied according to equation (1).

$$\mathbf{B}_{Tc} = \mathbf{B}_T + \left(\overline{B}_B - \mathbf{B}_B\right), \quad (1)$$

Where:

$\mathbf{B}_{Tc}$ = Corrected airborne total field readings

$\mathbf{B}_T$ = Airborne total field readings

$\overline{B}_B$ = Average datum base level

$\mathbf{B}_B$ = Base station readings

The average datum base level ($\overline{B}_{\mathrm{B}}$ **)** was set to 53596 nT for the data flown in 2019 from Alteidet, and at 53352 nT for the data flown in 2014 from Ystneset near Øksfjord community center.

Corrections for lag and heading

Neither a lag nor a cloverleaf test was performed before the survey. According to previous reports the lag between logged magnetic data and the corresponding navigational data was 1-2 fiducials. These values were observed to have a negligible effect on the processed results. A heading error for a towed system is usually either very small or non-existent. No lag and heading corrections were applied.

Magnetic data processing, gridding, and presentation

The total field magnetic anomaly data ($\mathbf{B}_{TA}$) were calculated from the diurnal corrected data ($\mathbf{B}_{Tc}$) after subtracting the IGRF for the surveyed area calculated for the data period (eq.2)

$$\mathbf{B}_{TA} = \mathbf{B}_{Tc} - IGRF \tag{2}$$

IGRF 2015 model was employed in these calculations, to ensure that the Øksfjord data set would match the previously processed and earlier published surrounding data sets.

The total field anomaly data were split into lines and then were gridded using a minimum curvature method with a grid cell size of 100 meters. This cell size is exactly one quarter of the 400 meters average line spacing. To remove small line-to-line levelling errors that were detected on the gridded magnetic anomaly data, the Geosoft micro-levelling technique was applied on the flight line based magnetic database. Then, the micro-leveled data was gridded using minimum curvature method with 100 meters grid cell size.

The processing steps of magnetic data presented so far, were performed on point basis. The following steps are performed on grid basis.

The horizontal and vertical gradient along with the tilt derivative of the total magnetic anomaly were calculated from the stitched micro-leveled total magnetic anomaly grid. The magnitude of the horizontal gradient was calculated according to equation (3)

$$HG = \sqrt{\left(\frac{\partial(B_{TA})}{\partial x}\right)^2 + \left(\frac{\partial(B_{TA})}{\partial y}\right)^2} \tag{3}$$

where $\mathbf{B}_{TA}$ is the micro-leveled total field anomaly field. The vertical gradient (VG) was calculated by applying a vertical derivative convolution filter to the micro-leveled $\mathbf{B}_{TA}$ field. The tilt derivative (TD) was calculated according to the equation (4)

$$TD = \tan^{-1}\left(\frac{VG}{HG}\right) \tag{4}$$

A 3x3 convolution filter was applied to smooth the resulted magnetic grids.

The results are presented in a series of colored shaded relief maps (1:100000). The maps are:

- Total field magnetic anomaly
- Horizontal gradient of total magnetic anomaly
- Vertical gradient of total magnetic anomaly
- Tilt derivative (or Tilt angle) of the total magnetic anomaly

These maps are representative of the distribution of magnetization over the surveyed areas. The list of the produced maps is shown in Table 6.

2.2 Electromagnetic data

The EM system transmits five fixed frequencies and records an in-phase (IP) and a quadrature (Q) response for each of the five coil sets of the electromagnetic system. The received signals are processed and used for calculation of apparent resistivity.

IP and Q data were filtered with 15 fiducial non-linear filter to eliminate spherical spikes, which were represented as irregular noise of large amplitude in records and high frequency noise of bird electronics. Then, a 20-fiducial low-pass filter was applied to suppress instrumental and cultural noise. These filters were not able to suppress all the noise. Also, shifts in IP and Q data, with amplitude of 5-10 ppm, was observed in some flights. These shifts were edited manually where possible.

To remove the effects of instrument drift caused by gradual temperature variations in the transmitting and receiving circuits, background responses are recorded during each flight. To obtain a background level, the bird is raised to an altitude of at least 1000 ft above the topographic surface so that no electromagnetic responses from the ground are present in the recorded traces.

The EM traces observed at this altitude correspond to a background (zero) level of the system. If these background levels are recorded at 20-30 minutes interval, then the linear drift of the system can be removed on a flight-by-flight basis, before any further processing is carried out. Geosoft HEM module was used for applying drift correction. Residual instrumental drift, usually small, but non-linear, was manually removed manually on a line-to-line basis.

When final levelling of the EM data was complete, apparent resistivity was calculated from in-phase and quadrature EM components using a homogeneous half space model of the earth (Geosoft HEM module) for 6600, 7000, 980, 880 and 34133 Hz. using threshold value of 2 ppm, starting value of 1000 ohm-m, and fractional error 1%.

Only the 2019 dataset includes 34 kHz EM data. The dataset from 2014 does not include 34 kHz EM data, thus it will appear as a gap in the map in figure 13.

Electromagnetic field decays rapidly with the distance (height of the sensors) – as z^{-2} – z^{-5} depending on the shape of the conductors and, at certain height, signals from the ground sources become comparable with instrumental noise. Levelling errors or precision of levelling can lead sometimes to appearance of artificial resistivity anomalies when data were collected at high instrumental altitude.

Application of threshold allows excluding such data from an apparent resistivity calculation, though not completely. It is particularly noticeable in low frequencies datasets. Resistivity data were visually inspected; artificial anomalies associated with high altitude measurements were manually removed.

Data recorded at a height higher than 150 meters were considered as non-reliable and removed from presentation. Final Apparent resistivity was gridded with a cell size 100 meters. Power lines strongly affected low frequency data – 880 and 980 Hz frequencies, and the most prominent noise from power lines were filtered manually.

2.3 Radiometric data

Airborne gamma-ray spectrometry measures the abundance of Potassium (K), Thorium (eTh), and Uranium (eU) in rocks, weathered materials and soil by detecting gamma-rays emitted due to the natural radioelement decay of these elements. The data analysis method is based on the IAEA recommended method for U, Th and K (International Atomic Energy Agency, 1991; 2003). A short description of the individual processing steps of that methodology as adopted by NGU is given bellow.

Energy windows
The Gamma-ray spectra were initially reduced into standard energy windows corresponding to the individual radio-nuclides K, U and Th. Figure 3 shows an example of a Gamma-ray spectrum and the corresponding energy windows and radioisotopes (with peak energy in MeV) responsible for the radiation.

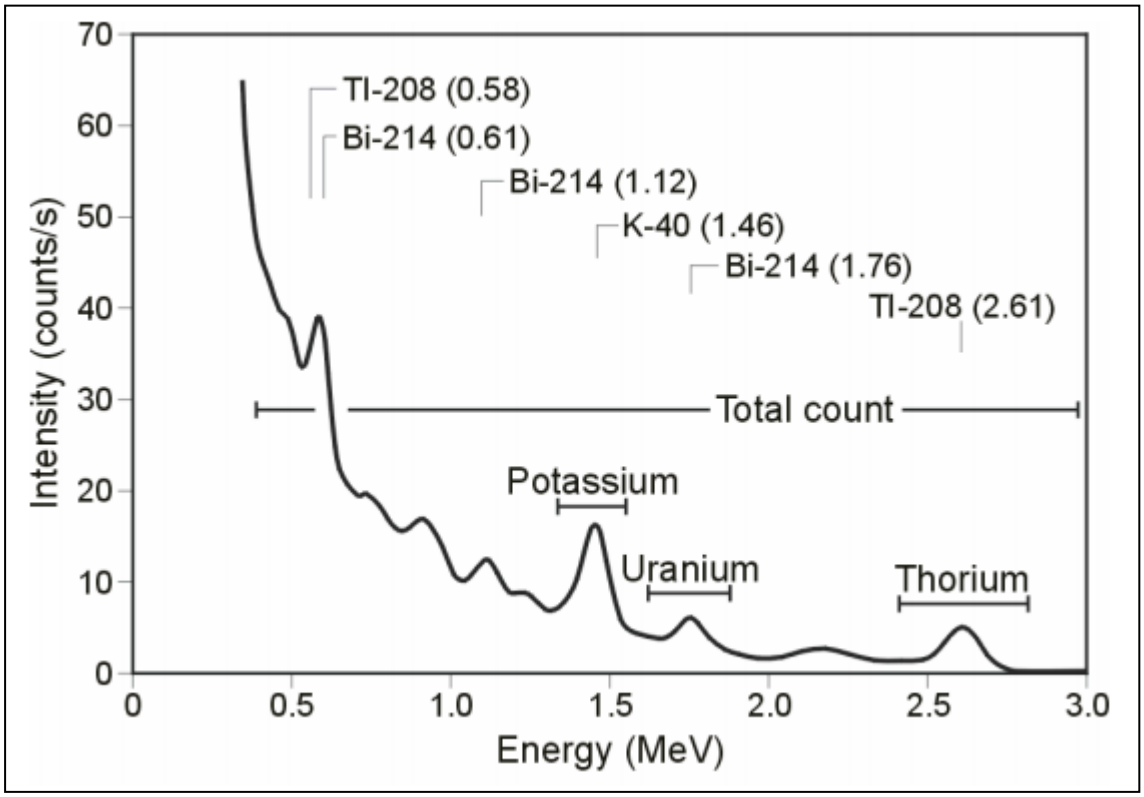

Figure 3: Gamma-ray spectrum with K, Th, U and Total Count windows

Table 5. Specified channel windows for the 1024 RSX-5 system.

Gamma-ray spectrum	Cosmic	Total count	K	U	Th
Down	1022	135-935	455-522	552-618	802-935
Up	1022			552-618	
Energy windows (MeV)	>3.07	0.4-2.8	1.36-1.56	1.65-1.85	2.4-2.8

The RSX-5 is a 1024 channel system with four downward and one upward looking detector, which means that the actual Gamma-ray spectrum is divided into 1024

channels. The first channel is reserved for the “Live Time” and the last for the Cosmic rays. Table 5 shows the windows that were used for the reduction of the spectrum.

Live Time correction

The data were corrected for live time. “Live time” is an expression of the relative length of time the instrument was able to register new pulses per sample interval. On the other hand, “dead time” is an expression of the relative length of time the system was unable to register new pulses per sample interval. The relation between “dead time” and “live time” is given by the equation (5)

“Live time” = “Real time” – “Dead time” (5)

where the “real time” or “acquisition time” is the elapsed time over which the spectrum is accumulated (about 1 second).

The live time correction is applied to the total count, Potassium, Uranium, Thorium, upward Uranium, and cosmic channels. The formula used to apply the correction is as follows:

$$C_{LT} = C_{RAW} \cdot \frac{Acquisition\ Time}{Live\ Time} \quad (6)$$

where C_{LT} is the live time corrected window in counts per second, C_{RAW} is the raw window data in counts per second, while Acquisition Time and Live Time are in microseconds.

Cosmic and aircraft correction

Background radiation resulting from cosmic rays and aircraft contamination was removed from the total count, Potassium, Uranium, Thorium, upward Uranium window using the following formula:

$$C_{CA} = C_{LT} - (a_c + b_c \cdot C_{Cos}) \quad (7)$$

where C_{CA} is the cosmic and aircraft corrected window, C_{LT} is the live time corrected window a_c is the aircraft background for this window, b_c is the cosmic stripping coefficient for this window and C_{Cos} is the low pass filtered cosmic window. Cosmic and aircraft background coefficients are determined by high altitude calibration flights.

Radon correction

The upward detector method, as discussed in IAEA (1991), was applied to remove the effects of the atmospheric radon in the air below and around the helicopter. Using spectrometry data over-water, where there is no contribution from the ground sources, enables the calculation of the coefficients (a_C and b_C) for the linear equations that relate the cosmic corrected counts per second of Uranium window with that of total count, Potassium, Thorium and Uranium upward window over water. Data over-land were used in conjunction with data over-water to calculate the a_1 and a_2 coefficients used in equation (8) for the determination of the Radon component in the downward Uranium window:

$$Radon_U = \frac{Uup_{CA} - a_1 \cdot U_{CA} - a_2 \cdot Th_{CA} + a_2 \cdot b_{Th} - b_U}{a_U - a_1 - a_2 \cdot a_{Th}} \quad (8)$$

where $Radon_u$ is the Radon component in the downward Uranium window, Uup_{CA} is the filtered upward uranium, U_{CA} is the filtered Uranium, Th_{CA} is the filtered Thorium, a_1, a_2, a_U and a_{Th} are proportional factors and b_U an b_{Th} are constants determined experimentally.

The effects of Radon in the downward Uranium are removed by simply subtracting $Radon_U$ from U_{CA}. The effects of radon in the other windows are removed using the following formula:

$$C_{RC} = C_{CA} - (a_C \cdot Radon_U + b_C) \tag{9}$$

where C_{RC} is the Radon corrected window, C_{CA} is the cosmic and aircraft corrected window, $Radon_U$ is the Radon component in the downward uranium window, a_C is the proportionality factor and b_C is the constant determined experimentally for this window from over-water data.

Compton stripping

Radon corrected Potassium, Uranium and Thorium windows are subjected to spectral overlap correction. Compton scattered gamma rays in the radio-nuclides energy windows were corrected by window stripping using Compton stripping coefficients determined from measurements on calibrations pads (Grasty et al, 1991) at the Geological Survey of Norway in Trondheim (see values in Appendix A2).

The stripping corrections are given by the following formulas:

$$A_1 = 1 - (g \cdot \gamma) - (\mathrm{a} \cdot \alpha) + (\mathrm{a} \cdot g \cdot \beta) - (b \cdot \beta) + (b \cdot \alpha \cdot \gamma) \tag{10}$$

$$U_{ST} = \frac{Th_{RC} \cdot ((g \cdot \beta) - \alpha) + U_{RC} \cdot (1 - b \cdot \beta) + K_{RC} \cdot ((b \cdot \alpha) - g)}{A_1} \tag{11}$$

$$Th_{ST} = \frac{Th_{RC} \cdot (1 - (g \cdot \gamma)) + U_{RC} \cdot (b \cdot \gamma - \mathrm{a}) + K_{RC} \cdot ((\mathrm{a} \cdot g) - b)}{A_1} \tag{12}$$

$$K_{ST} = \frac{Th_{RC} \cdot ((\alpha \cdot \gamma) - \beta) + U_{RC} \cdot ((\mathrm{a} \cdot \beta) - \gamma) + K_{RC} \cdot (1 - (\mathrm{a} \cdot \alpha))}{A_1} \tag{13}$$

where U_{RC}, Th_{RC}, K_{RC} are the Radon corrected Uranium, Thorium and Potassium and a, b, g, α, β, γ are Compton stripping coefficients, determined from measurements on calibration pads at NGU. U_{ST}, Th_{ST} and K_{ST} are stripped values of Uranium, Thorium and Potassium.

Reduction to Standard Temperature and Pressure

The radar altimeter data were converted to effective height (H_{STP}) using the acquired temperature and pressure data, according to the expression:

$$H_{STP} = H \cdot \frac{273.15}{T + 273.15} \cdot \frac{P}{1013.25} \tag{14}$$

where H is the smoothed observed radar altitude in meters, T is the measured air temperature in degrees Celsius and P is the measured barometric pressure in millibars.

Height correction
Variations caused by changes in the aircraft altitude relative to the ground were corrected to a nominal height of 60 meters. Data recorded at a height higher than 150 meters were considered as non-reliable and removed from processing. Total count, Uranium, Thorium and Potassium stripped windows were subjected to height correction according to the equation:

$$C_{60m} = C_{ST} \cdot e^{C_{ht} \cdot (60 - H_{STP})} \quad (15)$$

where C_{ST} is the stripped corrected window, C_{ht} is the height attenuation factor for that window, determined from calibration flights, and H_{STP} is the effective height.

Conversion to ground concentrations
Finally, corrected count rates were converted to effective ground element concentrations using calibration values derived from calibration pads (Grasty et al, 1991) at the Geological Survey of Norway in Trondheim (see values in Appendix A2). The corrected data provide an estimate of the apparent surface concentrations of Potassium, Uranium and Thorium (K, eU and eTh). Potassium concentration is expressed as a percentage, equivalent Uranium and Thorium as parts per million (ppm). Uranium and Thorium are described as “equivalent” since their presence is inferred from gamma-ray radiation from daughter elements (^{214}Bi for Uranium, ^{208}TI for Thorium). The concentration of the elements is calculated according to the following expressions:

$$C_{CONC} = C_{60m} / C_{SENS\_60m} \quad (16)$$

where C_{60m} is the height corrected window, C_{SENS_60m} is experimentally determined sensitivity reduced to the nominal height (60m).

Spectrometry data gridding and presentation
Gamma-rays from Potassium, Thorium and Uranium emanate from the uppermost 30 to 40 centimeters of soil and rock in the crust (Minty, 1997). Variations in the concentrations of these radioactive elements are largely related to changes in the mineralogy and geochemistry of the Earth’s surface.

The spectrometry data were stored in a database and the ground concentrations were calculated following the processing steps. A list of the parameters used in these steps is given in Appendix A3.

Then the data were split in lines and ground concentrations of the three main natural radio-elements Potassium, Thorium and Uranium and total gamma-ray flux (total count) were gridded using a minimum curvature method with a grid cell size of 100 meters. To remove small line-to-line levelling errors appeared on those grids, the data were micro-leveled as in the case of the magnetic data, and re-gridded with the same grid cell size.

Quality of the radiometric data was within standard NGU specifications (Rønning 2013). For further reading regarding standard processing of airborne radiometric data, we recommend the publications from Minty et al. (1997). A 3x3 convolution filter was applied to smooth the concentration grids. A list of the produced maps is shown in Table 6.

3. PRODUCTS

Processed digital data from the survey are presented as:

1. Geosoft XYZ files: Oksfjord_Mag.xyz, Oksfjord_EM.xyz, Oksfjord_Rad.xyz, Colored maps at the scale 1:100000 available from NGU on request.

2. Grid-files in Geo-TIFF format

Table 6. Maps in scale 1:100000, available from NGU on request.

Map #	Name
2022.013-00	Survey Flight Path
2022.013-01	Total magnetic field
2022.013-02	Magnetic Horizontal Gradient
2022.013-03	Magnetic Vertical Gradient
2022.013-04	Magnetic Tilt Derivative
2022.013-05	Apparent resistivity, Frequency 7000 Hz, coaxial coils
2022.013-06	Apparent resistivity, Frequency 6600 Hz, coplanar coils
2022.013-07	Apparent resistivity, Frequency 980 Hz, coaxial coils
2022.013-08	Apparent resistivity, Frequency 880 Hz, coplanar coils
2022.013-09	Apparent resistivity, Frequency 34133 Hz, coplanar coils
2022.013-10	Radiometric Total counts
2022.013-11	Potassium ground concentration
2022.013-12	Uranium ground concentration
2022.013-13	Thorium ground concentration
2022.013-14	Radiometric Ternary Image

Downscaled images of the maps are shown in figures 4 to 18.

4. REFERENCES

IAEA 1991: Airborne Gamma-Ray Spectrometry Surveying, Technical Report No 323, Vienna, Austria, 97 pp

Geotech 1997: Hummingbird Electromagnetic System. User manual. Geotech Ltd. October 1997

Grasty, R.L., Holman, P.B. & Blanchard 1991: Transportable Calibration pads for ground and airborne Gamma-ray Spectrometers. Geological Survey of Canada. Paper 90-23. 62 pp.

IAEA 2003: Guidelines for radioelement mapping using gamma ray spectrometry data. IAEA-TECDOC-1363, Vienna, Austria. 173 pp.

Minty, B.R.S., Luyendyk, A.P.J. and Brodie, R.C. 1997: Calibration and data processing for gamma-ray spectrometry. AGSO – Journal of Australian Geology & Geophysics. 17(2). 51-62.

Naudy, H. and Dreyer, H. 1968: Non-linear filtering applied to aeromagnetic profiles. Geophysical Prospecting. 16(2). 171-178.

Rønning, J.S. 2013: NGUs helikoptermålinger. Plan for sikring og kontroll av datakvalitet. NGU Intern rapport 2013.001, (38 sider).

Appendix A1: Flow chart of magnetic processing

Meaning of parameters is described in the referenced literature.

Processing flow:

- Creation of database and quality control.
- Visual inspection of airborne data and manual spike removal
- Import of diurnal data from base magnetometer database.
- Correction of data for diurnal variation.
- IGRF 2015 removed.
- Splitting flight data by lines
- Gridding
- Microlevelling
- 3x3 convolution filter

Appendix A2: Flow chart of EM processing

Meaning of parameters is described in the referenced literature.

Processing flow:

- Automated leveling using Geosoft HEM module
- Filtering of in-phase and quadrature channels with non-linear and low-pass filters
- Quality control and visual inspection of data.
- Manual removal of remaining part of instrumental drift
- Additional levelling using low-pass filter to reduce linear noise
- Calculation of an apparent resistivity using in-phase and quadrature channels.
- Splitting flight data by lines
- Gridding

Appendix A3: Flow chart of radiometry processing

Underlined processing stages are not only applied to the K, U and Th window, but also to the total count. Meaning of parameters is described in the referenced literature. The 2014 and 2019 surveys used different spectrometers, so the data have been processed with separate set of coefficients.

- Airborne and cosmic correction (IAEA, 2003)
  Used parameters: determined by high altitude calibration flights (1500-9000 ft) at Frosta in January 2014. Coefficients used for data flown in 2014.

Window	Background	Cosmic
K	5.3584	0.057
U	1.427	0.0467
Th	0	0.0448
Uup	0.7051	0.0643
Total counts	42.726	1.0317

  Used parameters: determined by high altitude calibration flights (1500-9000 ft) at Langøya in 2013. Coefficients used for data flown in 2019.

Window	Background	Cosmic
K	7.3314	0.0617
U	0.7369	0.0475
Th	0	0.0647
Uup	0.3927	0.0423
Total counts	36.291	1.0397

- Radon correction using upward detector method (IAEA, 2003)
  Used parameters determined from survey data over water and land at Øksfjord 2014:

Coefficient	Value	Coefficient	Value
a_u	0.18499	$\mathbf{b_u}$	0.1889
a_K	0.31435	$\mathbf{b_K}$	3.29311
a_{Th}	0.10767	$\mathbf{b_{Th}}$	0.87095
a_{TC}	8.26977	$\mathbf{b_{TC}}$	30.85087
a_1	0.04615131	$\mathbf{a_2}$	0.041221219

- Radon correction using upward detector method (IAEA, 2003)
  Used parameters determined from survey data over water and land at Øksfjord 2019:

Coefficient	Value	Coefficient	Value
a_u	0.21828	$\mathbf{b_u}$	0.38793
a_K	0.89064	$\mathbf{b_K}$	2.2319
a_{Th}	0.02918	$\mathbf{b_{Th}}$	0.3471
a_{TC}	13.53163	$\mathbf{b_{TC}}$	18.51517
a_1	0.06829369	$\mathbf{a_2}$	0.03240899

- Stripping corrections (IAEA, 2003)
  Used parameters determined from measurements on calibrations pads at NGU, June 5th 2014 for the 2014 data, and May 20th 2020 for the 2019 data.

Coefficient	**2014 Stripping factors**	**2019 Stripping factors**
a	0.047186	0.04786
b	0	0
c	0	0
α	0.305607	0.30649
β	0.484063	0.47097
γ	0.814612	0.82207

- Height correction to a height of 60 m
  Parameters determined by high altitude calibration flights (100 – 700 ft). The average values from tests performed at Frosta in January 2014 was used for 2014 data, and from Beitostølen, 2015 was used for 2019 data. Attenuation factors in 1/m:

Window	**2014 Attenuation factors**	**2019 Attenuation factors**
K	-0.00888	-0.010136
U	-0.00653	-0.00842
Th	-0.00662	-0.008348
TC	-0.00773	-0.009431

- Converting counts at 60 m heights to element concentration on the ground
  Used parameters determined from measurements on calibrations pads at NGU.

Window	**2014 Sensitivity**	**2019 Sensitivity**
K (%/count)	0.007480	0.007574
U (ppm/count)	0.087599	0.088361
Th (ppm/count)	0.156147	0.152853

- Microlevelling using Geosoft menu and smoothening by a convolution filtering.

Microlevelling parameters	**Value**
De-corrugation cutoff wavelength (m)	1200
Cell size for gridding (m)	50
Naudy (1968) Filter length (m)	800

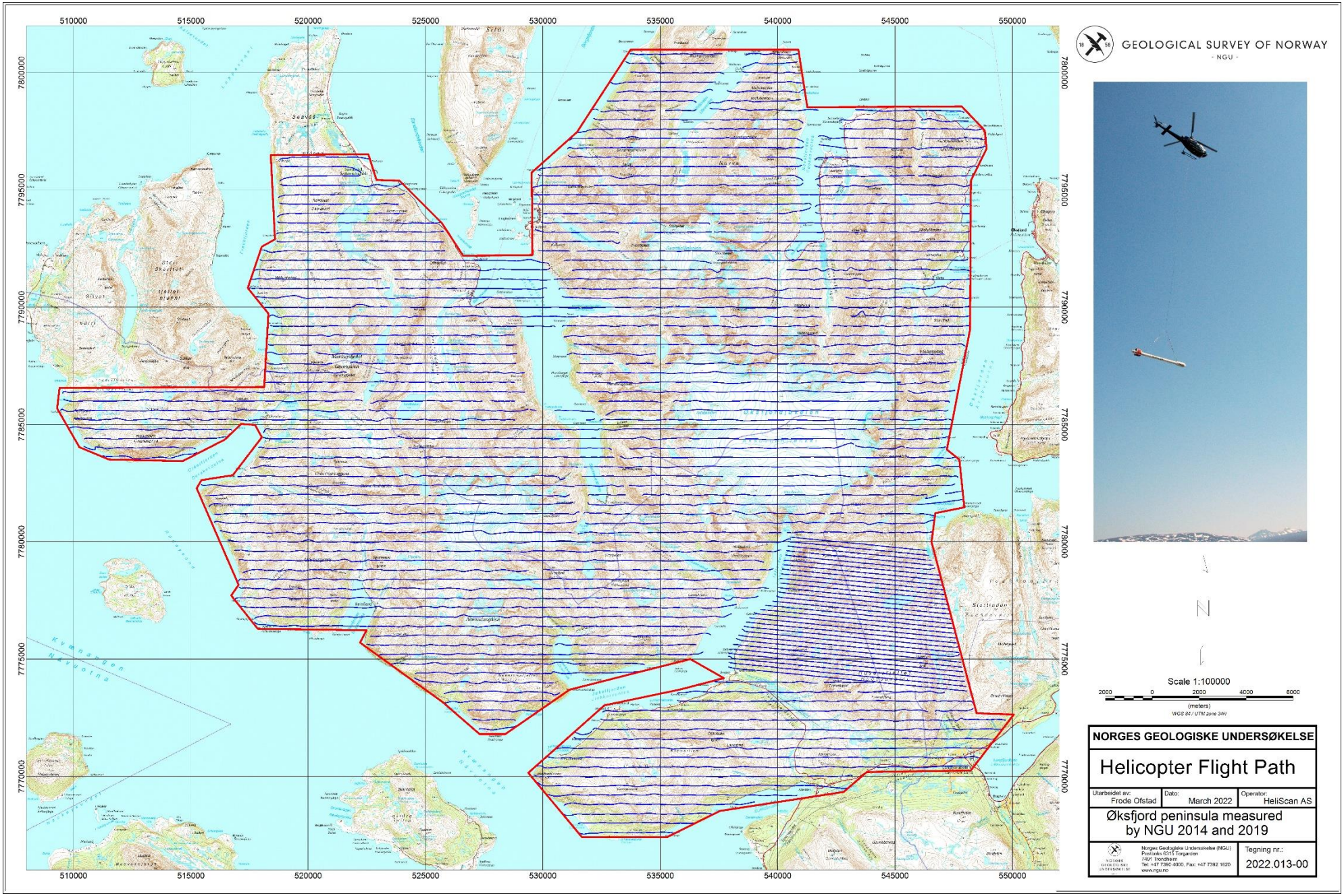

Figure 4: Øksfjord survey area with flight path

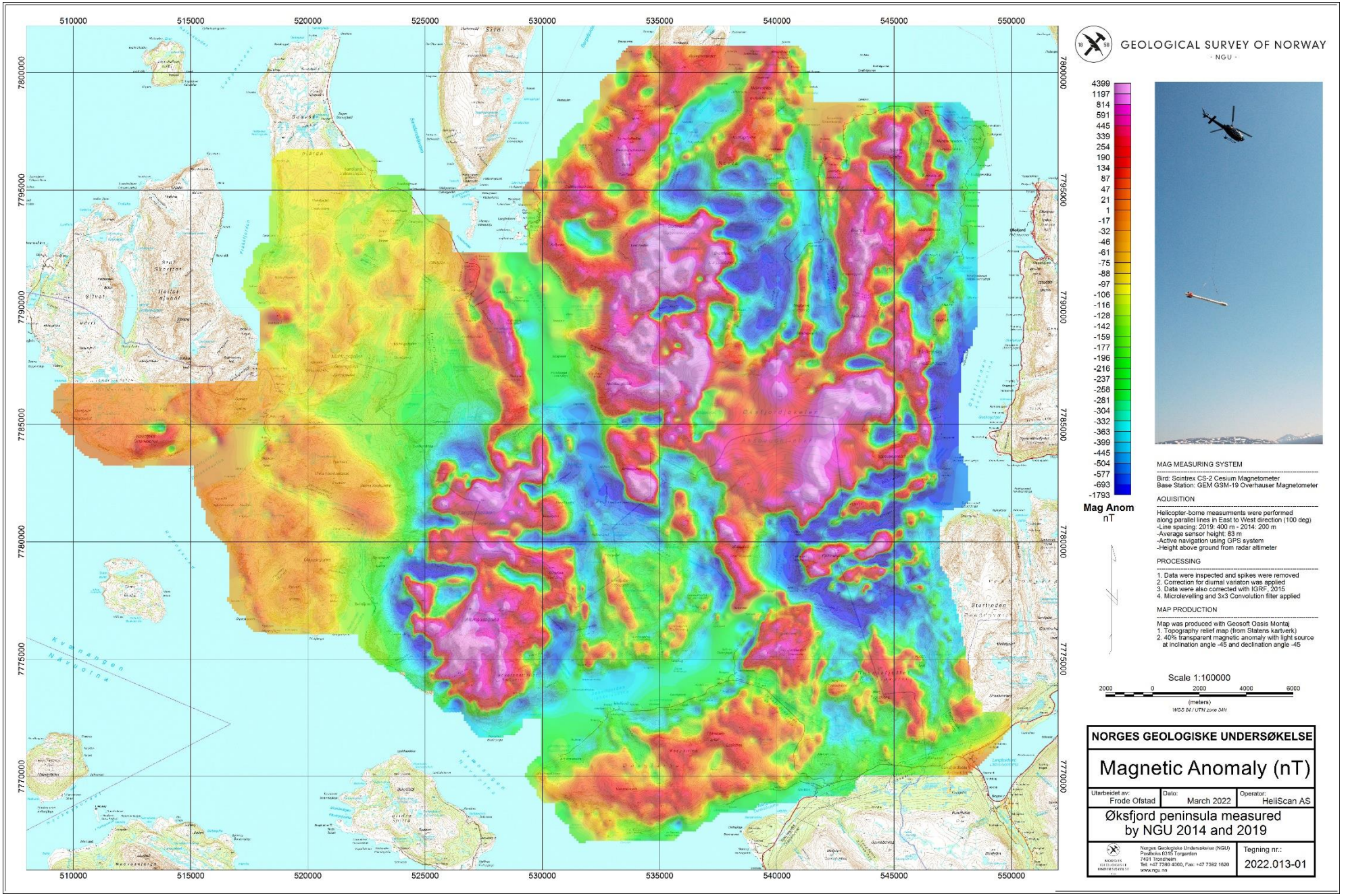

Figure 5: Total Magnetic Field

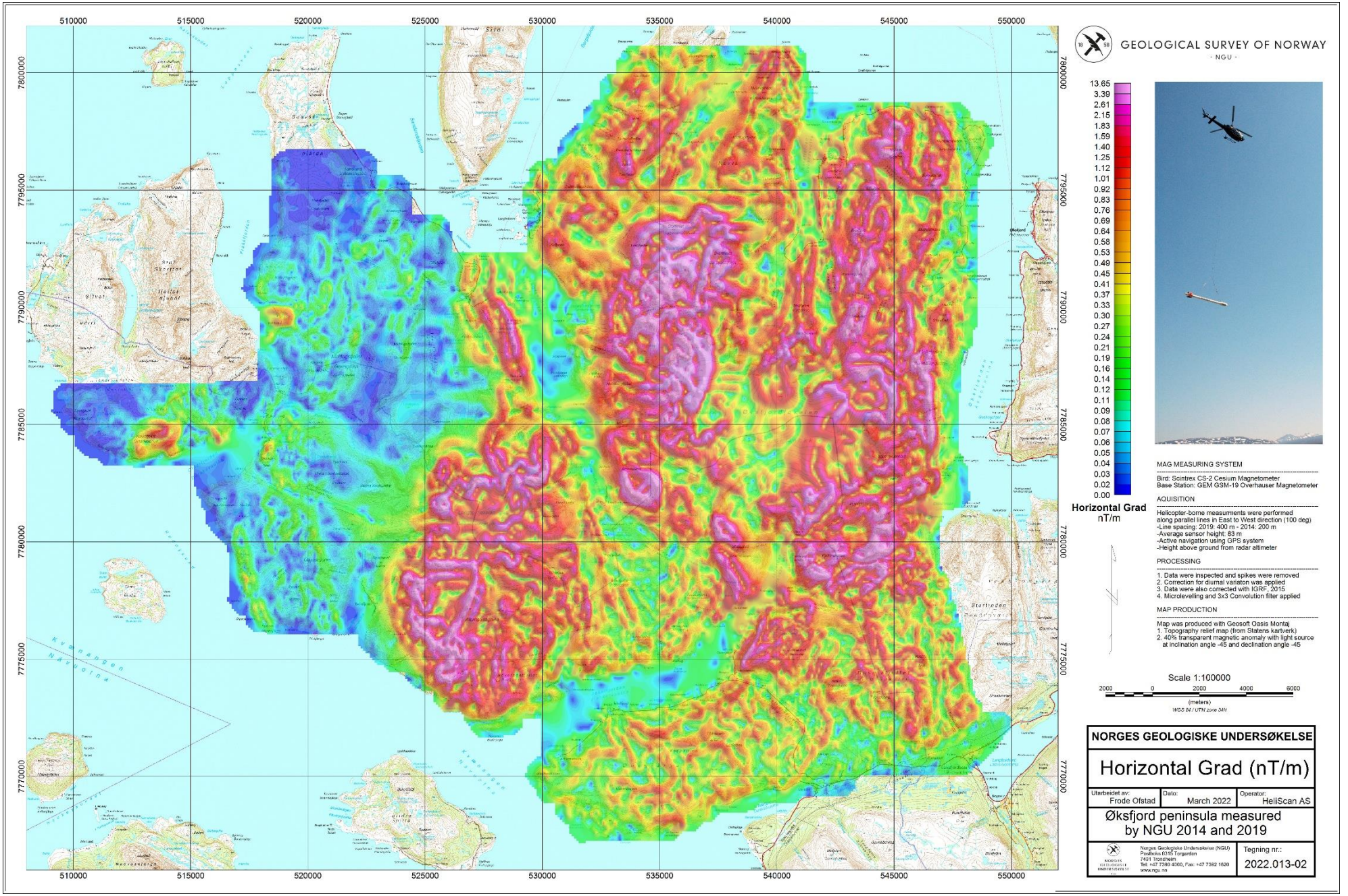

Figure 6: Magnetic Horizontal Gradient

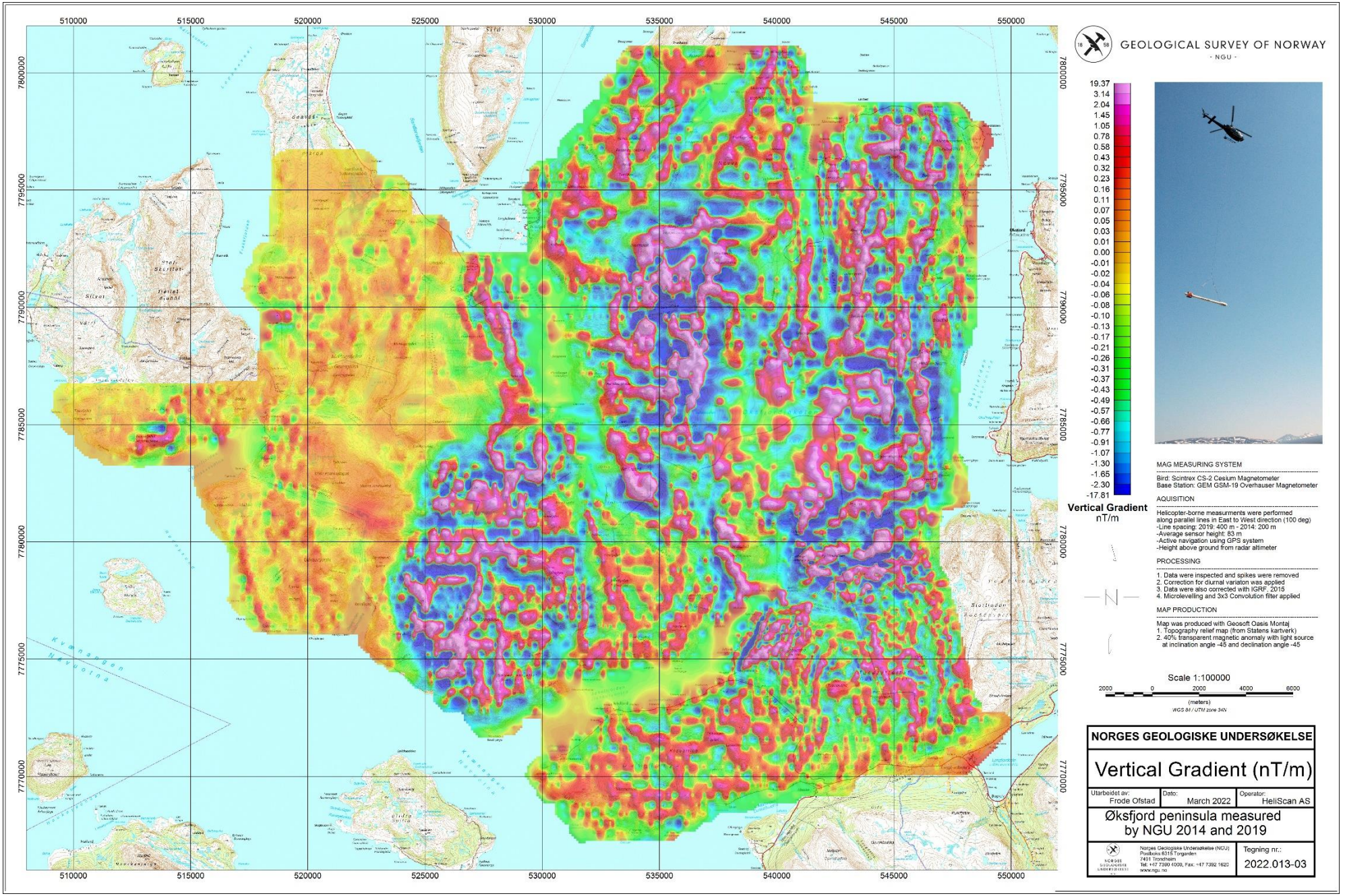

Figure 7: Magnetic Vertical Gradient

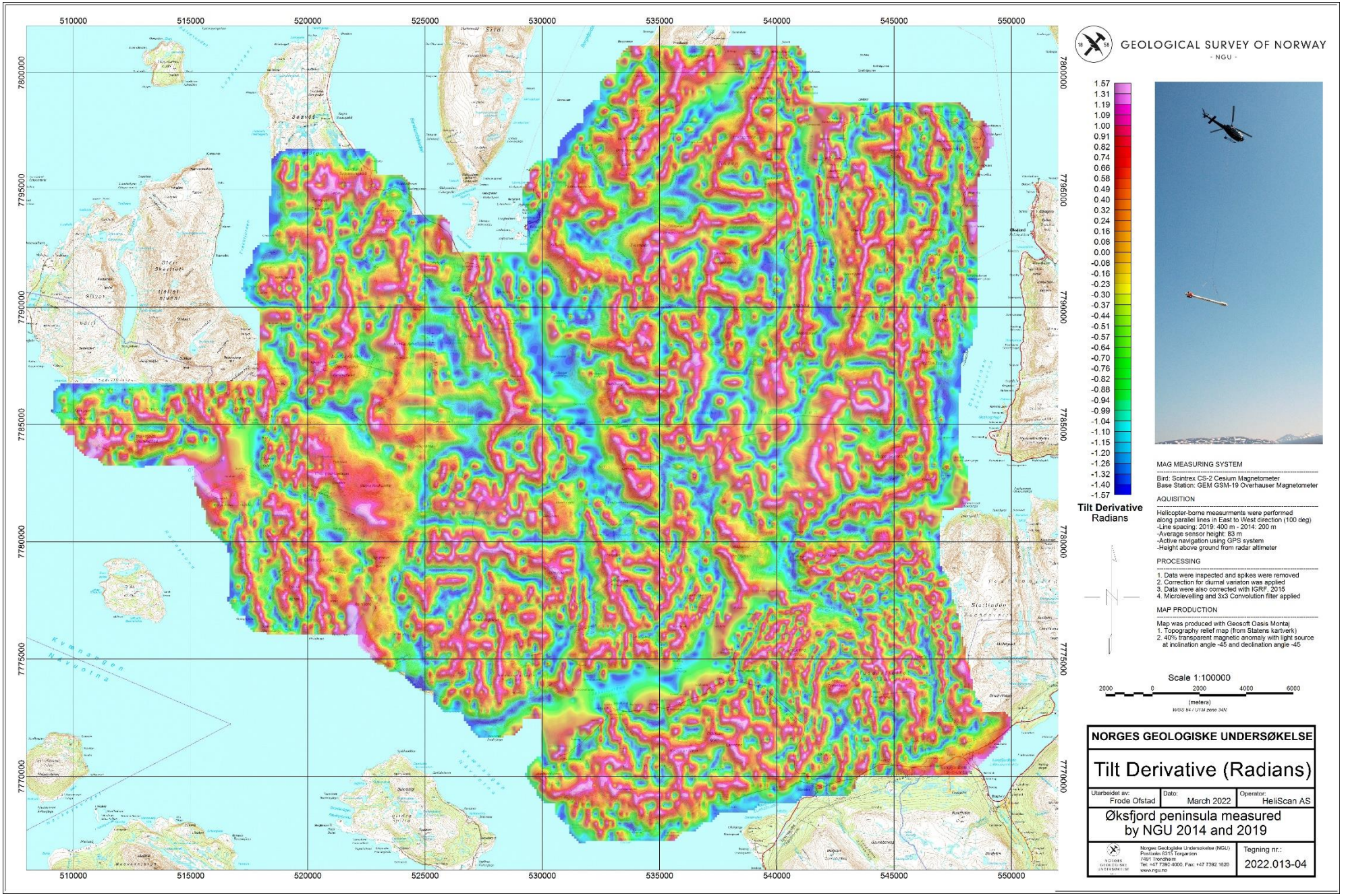

Figure 8: Magnetic Tilt Derivative

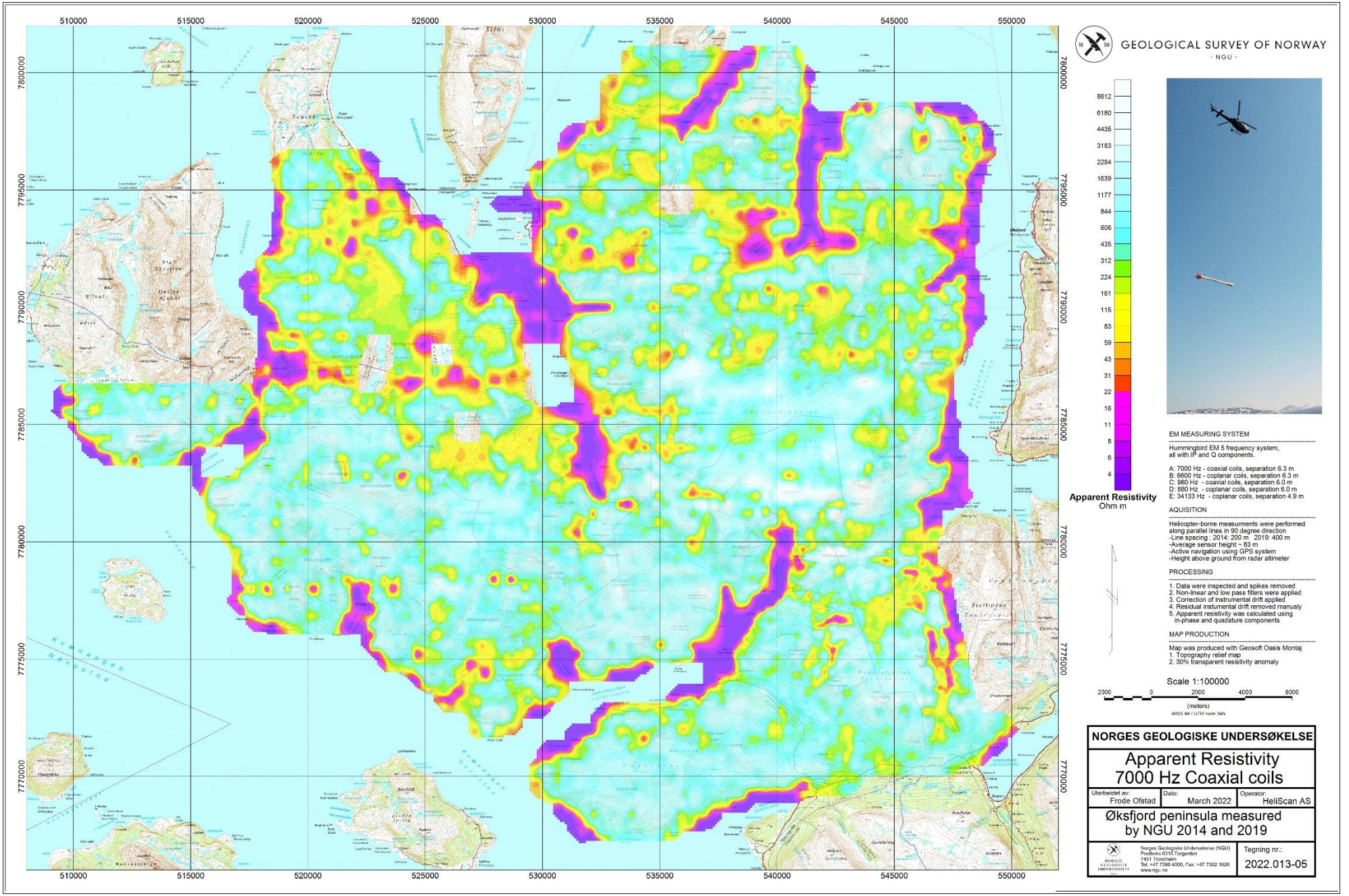

Figure 9: Apparent resistivity. Frequency 7000 Hz, Coaxial coils

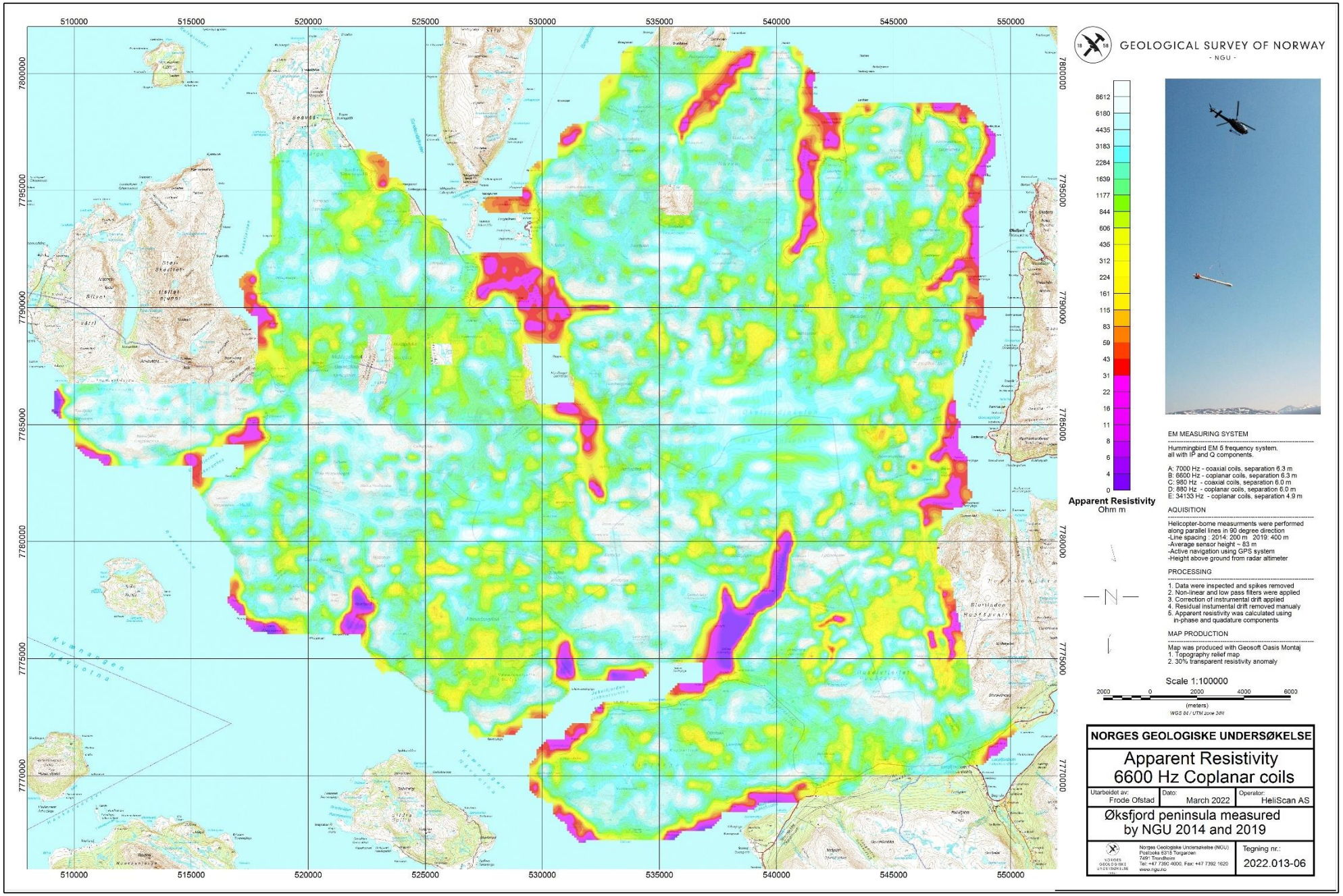

Figure 10: Apparent resistivity. Frequency 6600 Hz, Coplanar coils

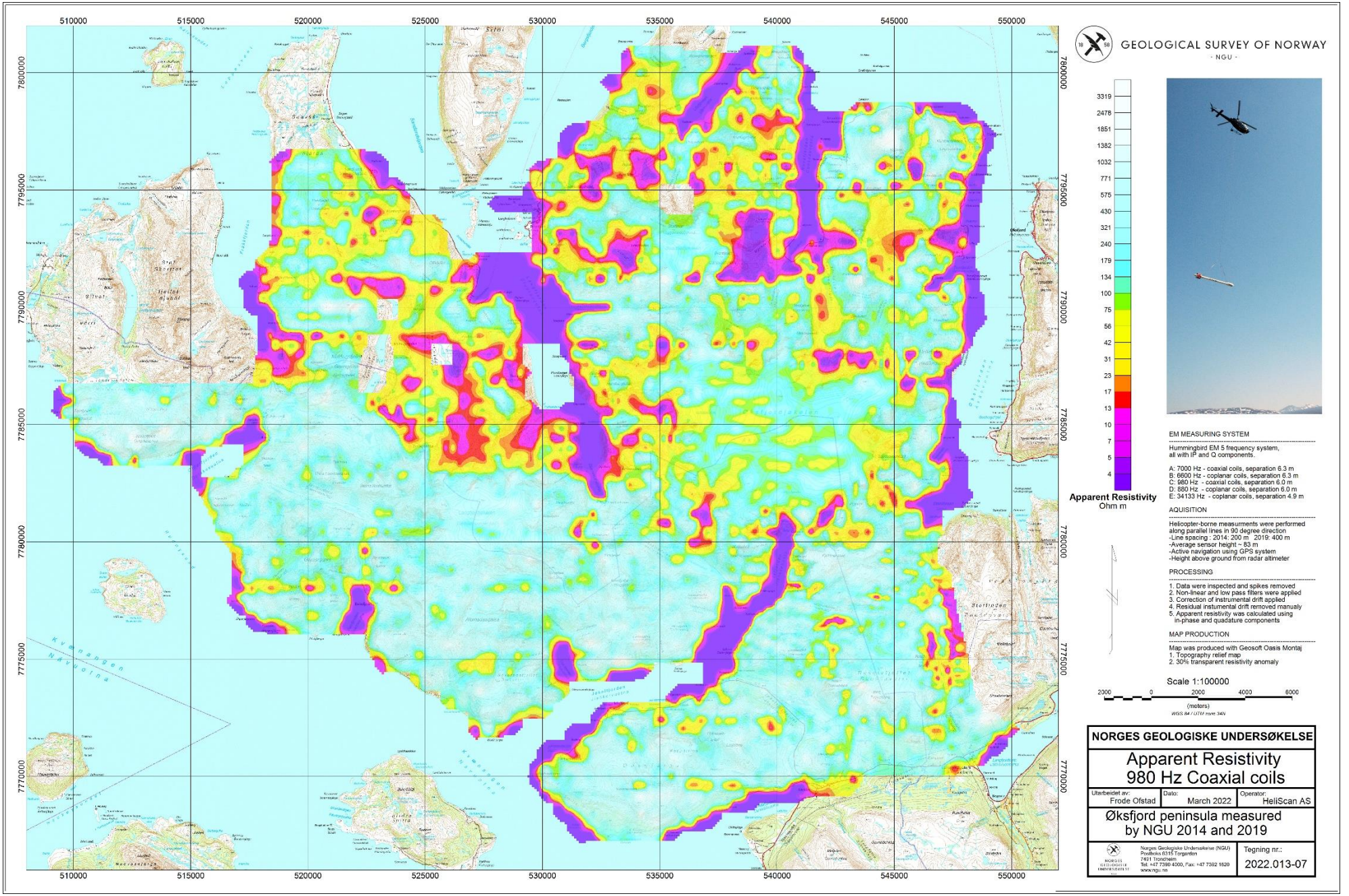

Figure 11: Apparent resistivity. Frequency 980 Hz, Coaxial coils

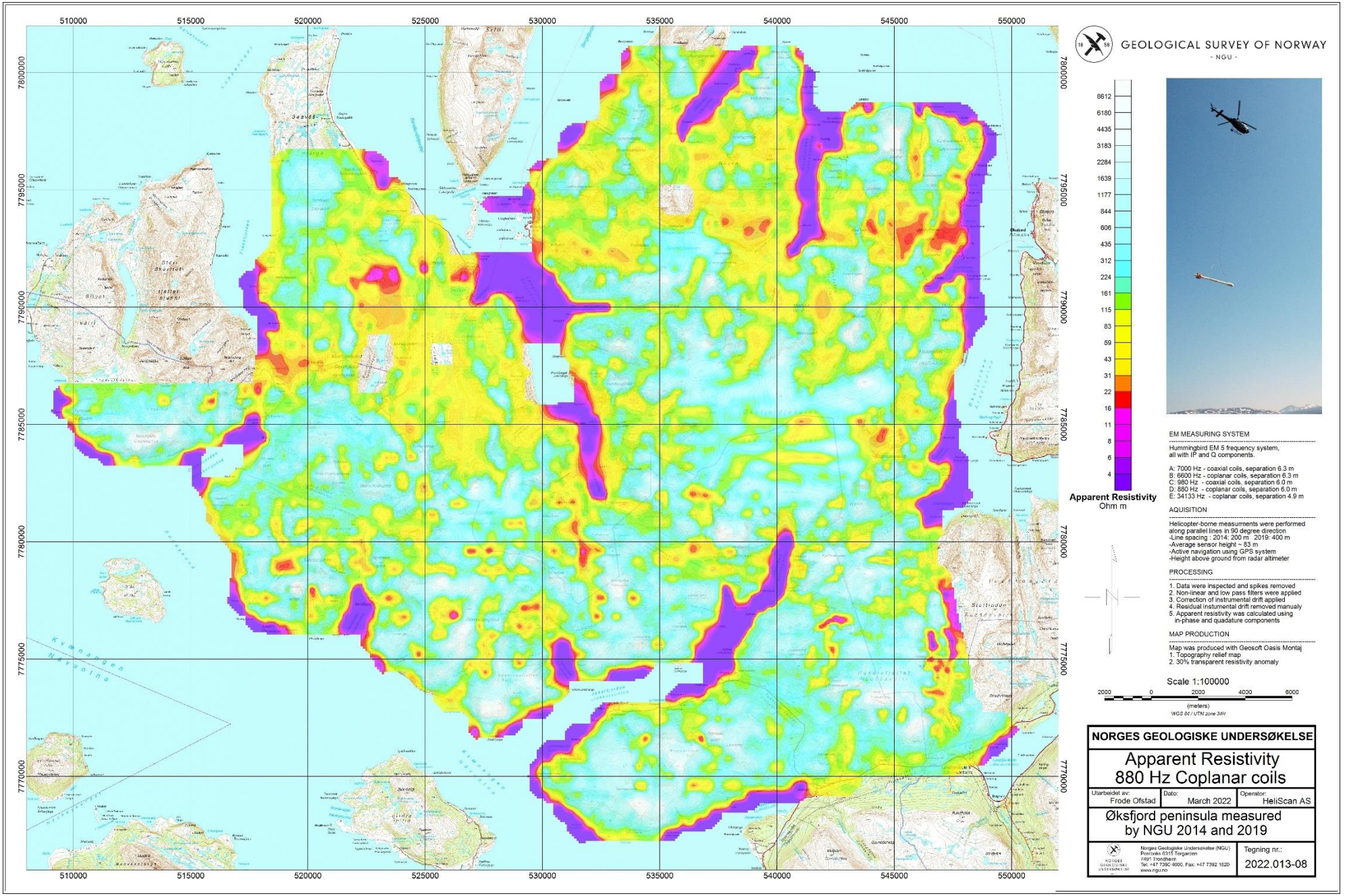

Figure 12: Apparent resistivity. Frequency 880 Hz, Coplanar coils

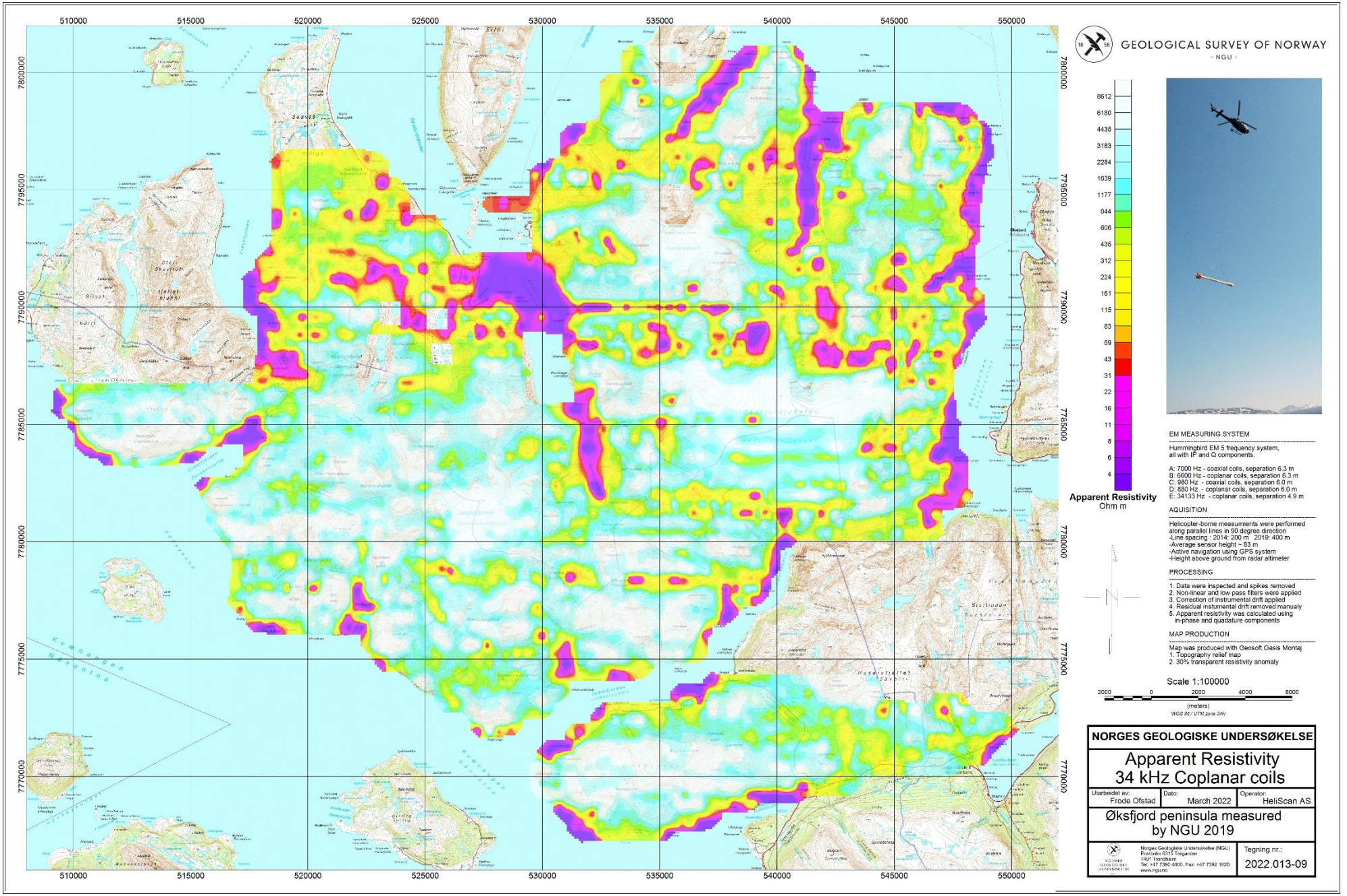

Figure 13: Apparent resistivity. Frequency 34133 Hz, Coplanar coils

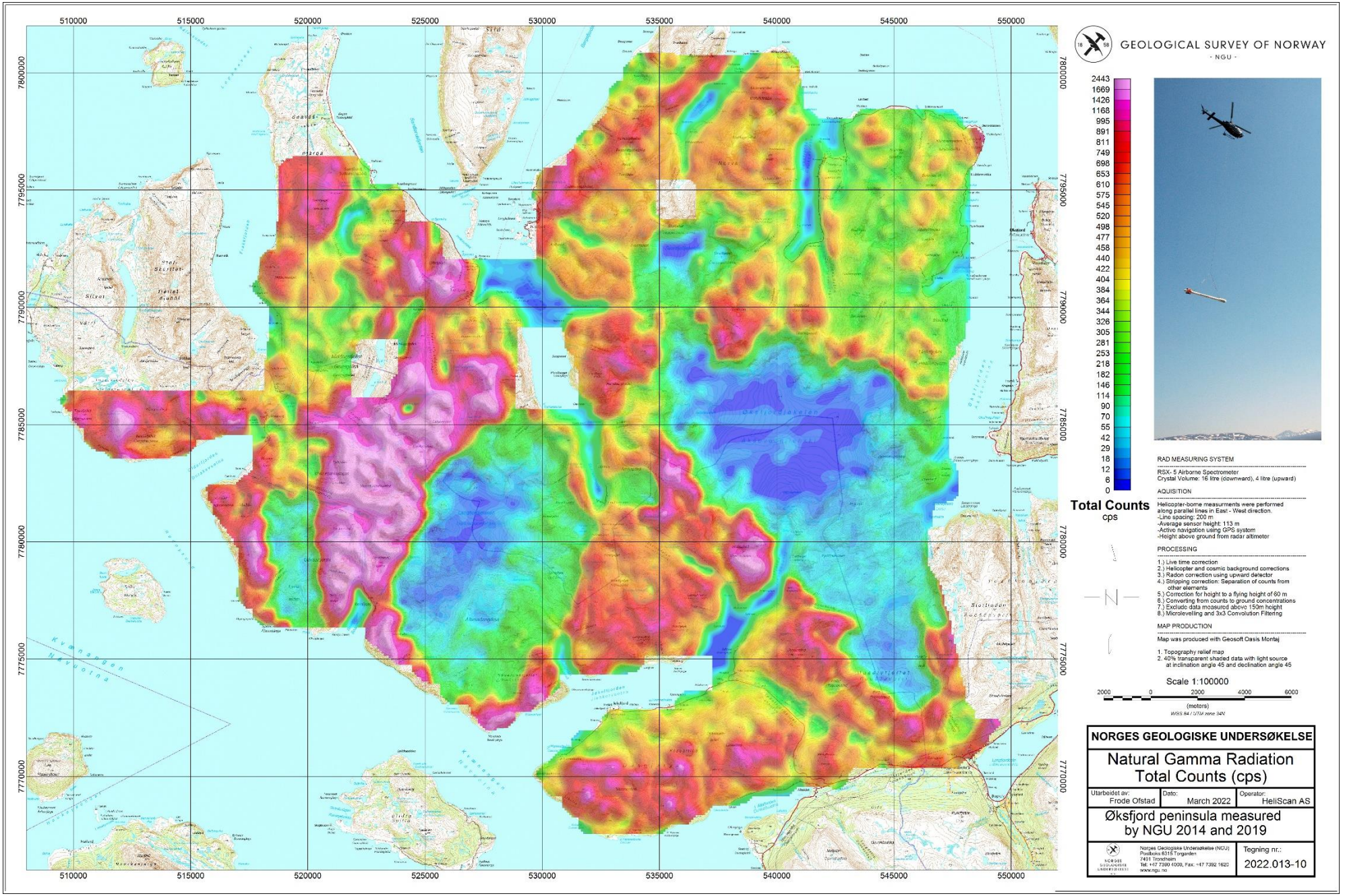

Figure 14: Radiometric Total Counts

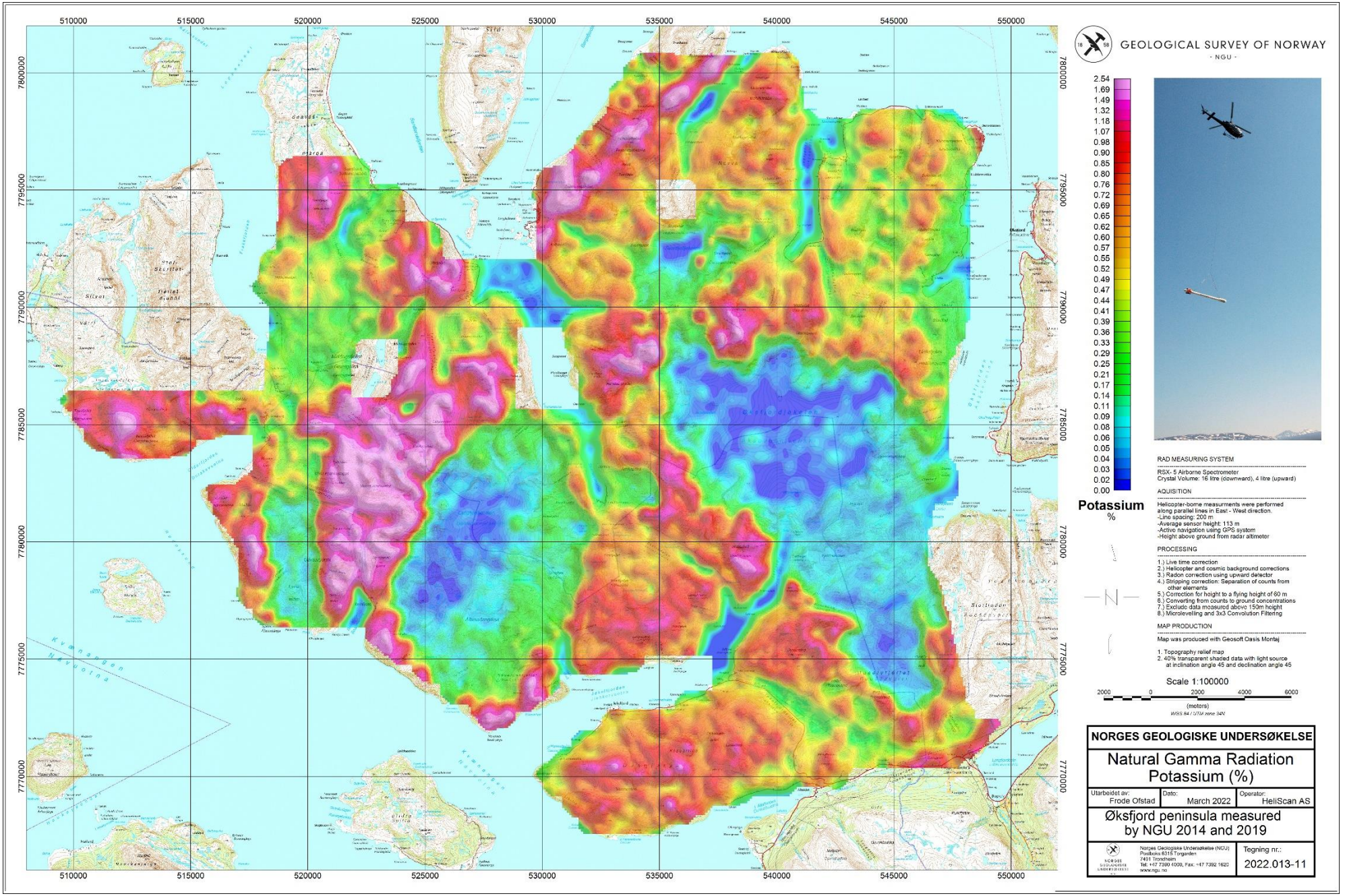

Figure 15: Potassium ground concentration

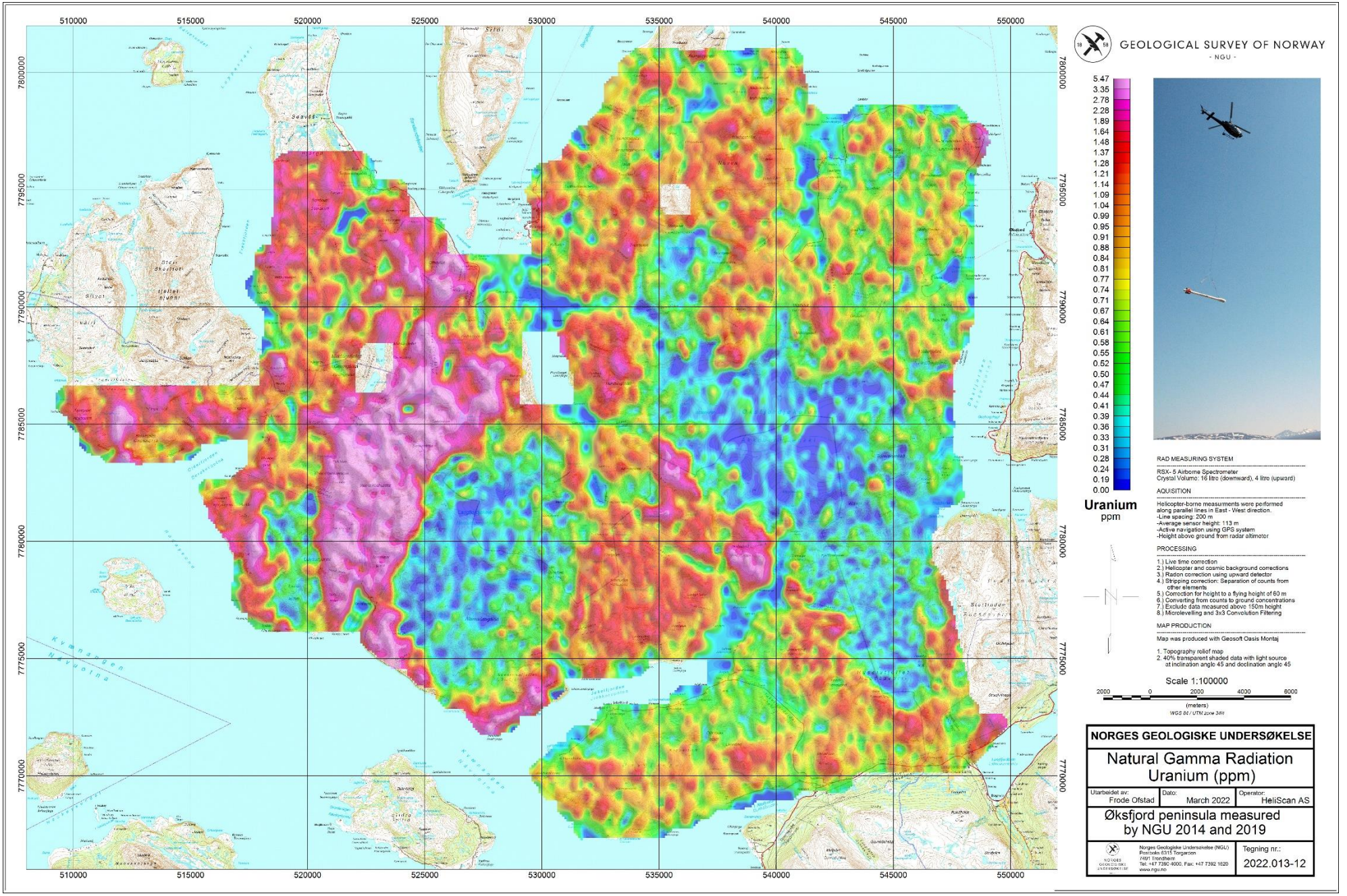

Figure 16: Uranium ground concentration

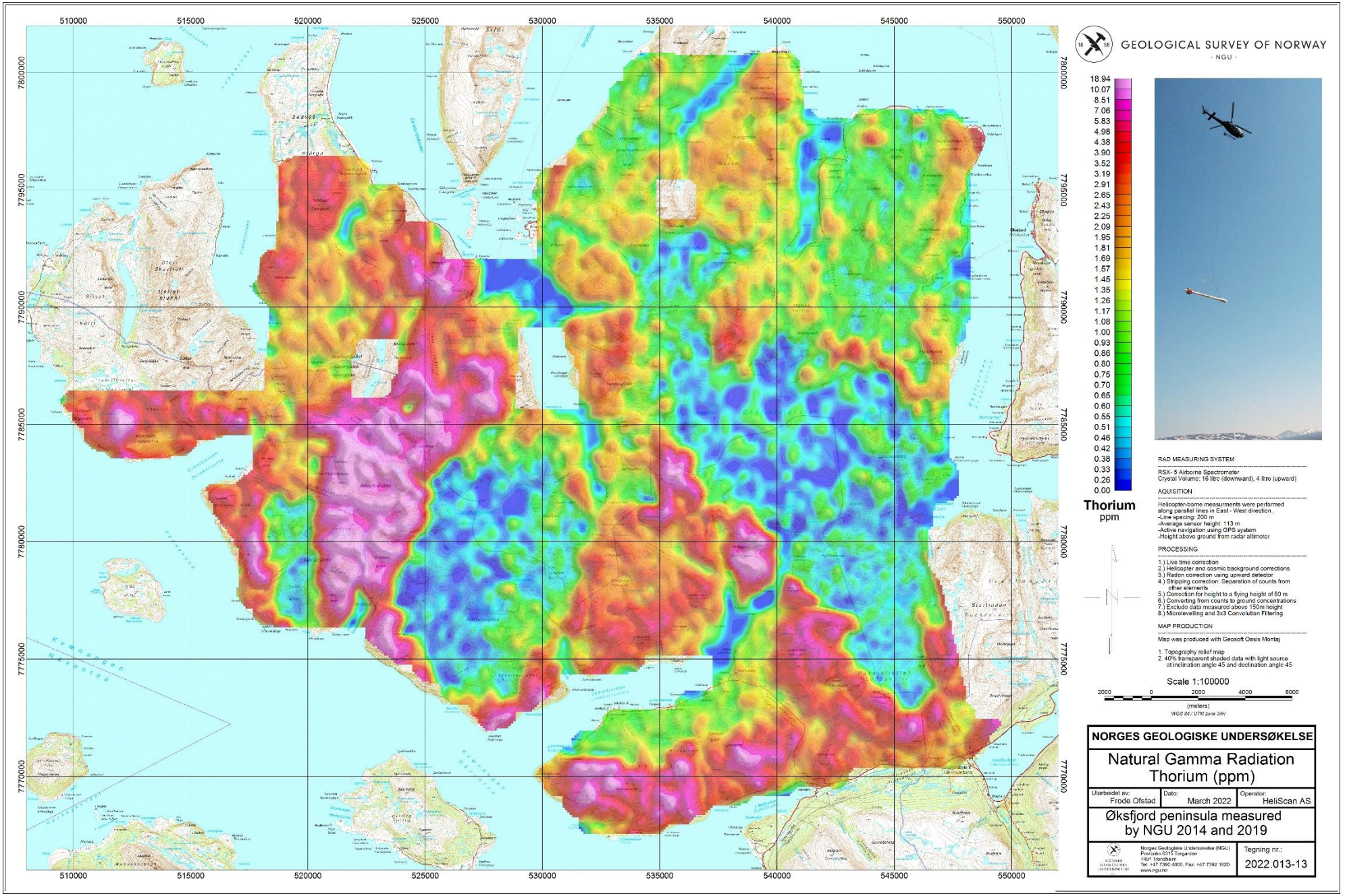

Figure 17: Thorium ground concentration

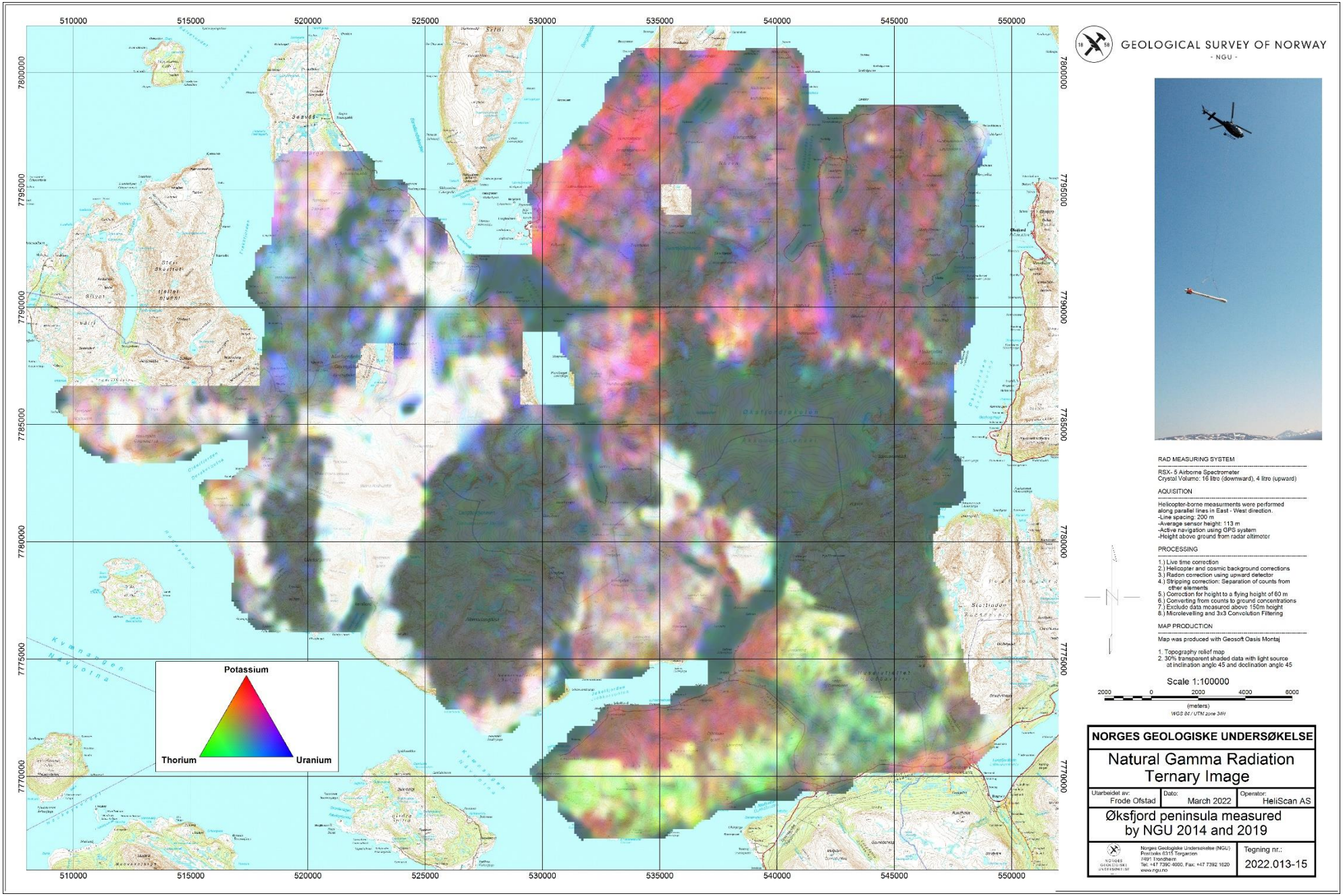

Figure 18: Radiometric Ternary Image

GEOLOGICAL
SURVEY OF
NORWAY

· NGU ·

Geological Survey of Norway
PO Box 6315, Sluppen
N-7491 Trondheim, Norway

Visitor address
Leiv Eirikssons vei 39
7040 Trondheim

Tel (+ 47) 73 90 40 00
E-mail ngu@ngu.no
Web www.ngu.no/en-gb/